

See discussions, stats, and author profiles for this publication at: <https://www.researchgate.net/publication/6883106>

# $\gamma$ -Radiation Induced Changes in the Physical and Chemical Properties of Lignocellulose

ARTICLE *in* BIOMACROMOLECULES · SEPTEMBER 2006

Impact Factor: 5.75 · DOI: 10.1021/bm060168y · Source: PubMed

---

CITATIONS

42

---

READS

150

3 AUTHORS, INCLUDING:



Ferdous Khan

KNAUF INSULATION LTD.

47 PUBLICATIONS 580 CITATIONS

SEE PROFILE

# $\gamma$ -Radiation Induced Changes in the Physical and Chemical Properties of Lignocellulose

Ferdous Khan,<sup>†</sup> S. R. Ahmad,\* and E. Kronfli

Department of Environmental and Ordnance Systems, Defence Academy of the UK, Cranfield University, Shrivenham, Swindon Wiltshire, SN6 8LA, U.K.

Received February 23, 2006; Revised Manuscript Received May 23, 2006

$\gamma$ -radiation induced effects on the physical and chemical properties of natural lignocellulose (jute) polymer were investigated. Samples were irradiated to required total doses at a particular dose rate. The changes in the parameters such as the tensile strength, elongation at break, and work done at rupture for the lignocellulose samples on irradiation with the  $\gamma$ -rays from a cobalt-60 source were measured. The mechanical properties were found to have nonlinear relations with the radiation doses. The chemical stability of irradiated fibers was found to degrade progressively with the increase of radiation dose. Additionally, other chemical changes of the samples due to exposure to high-energy radiation were also investigated using fluorescence and infrared spectroscopic analysis. Differential scanning calorimetry and thermogravimetric studies showed a significant reduction in thermal stability. The wide-angle X-ray diffraction study showed that structural changes of cellulose appeared due to the radiation-induced chemical reaction of lignocellulose.

## Introduction

Jute, a biodegradable natural lignocellulose fiber, contains approximately 58–63% cellulose, 20–24% hemicelluloses, and 12–15% lignin, in addition to small quantities of protein, pectin, wax and fats, acetyl content, mineral matter, and traces of pigments. The lignin in jute is a complex hydrocarbon polymer with both aliphatic and aromatic constituents. The hemicelluloses contain several different sugar units having a considerable degree of chain branching. The cellulose is a linear polymer of cellobiose repeating unit, and the degree of polymerization is normally 10 to 100 times greater than that of hemicelluloses. The lignin and hemicellulose molecules are linked through ester linkages formed by the carboxyl groups in the lignin.<sup>1</sup> This linkage governs the physical properties of jute fibers.

The effect of  $\gamma$ -radiation on natural cellulose other than jute has been the subject of extensive research over the past few decades.<sup>2,3</sup> The radiation-induced reactions in the macromolecules of the cellulose materials are known to be initiated through rapid localization of the absorbed energy within the molecules to produce long- and short-lived radicals. The cellulose contains carbon, oxygen, and hydrogen atoms, and each atom of this unit has practically equal probability of being ionized to take part in chemical reactions such as chain scission, cross-linking, and so forth. The efficiency of these two types of reactions depends mainly on the polymer structure and radiation dose.<sup>4</sup> The radiation effects on the physical, chemical, and biological properties of other polymers have been studied extensively.<sup>4–14</sup> Several studies<sup>5,7,10,11</sup> have shown that the irradiation of cotton cellulose deteriorated the mechanical parameters due to the chain scission reaction within the cellulose molecules. Takács and co-workers<sup>15–17</sup> have reported that the high-energy radiation cause a decrease in the degree of polymerization and an increase in the carbonyl content of cotton cellulose. Similar studies have, so far, not been reported on jute

fiber. To determine the truly definite mechanisms for the radiation chemistry of jute, both the chemical and physical properties after radiation need to be studied. Therefore, considering the importance of jute as a cheap, renewable, and biodegradable substitute for synthetic polymers, it is considered prudent to undertake this study.

## Experimental Section

**Materials.** Jute fibers were obtained from Amin Jute Mills Co., Dhaka, Bangladesh, and stored at the ambient laboratory atmospheric conditions. The bark materials from the fibers were removed, and the fibers were extracted by refluxing in a Soxhlet apparatus, using methanol as a solvent. The refluxing was conducted over a 72-h period, following which these were dried at 40 °C in a vacuum environment. About 2 g of fiber were weighed and arranged into an array having an average length of 150 mm and compressed between two hard boards to obtain a sample thickness of 5 mm or less. These were then exposed to a <sup>60</sup>Co- $\gamma$  radiation source in air. At halfway through the irradiation period, the samples were turned through a 180° angle to provide uniform irradiation throughout the bulk of the sample.

**Characterization Methods. Mechanical Properties.** The mechanical properties were analyzed using a microprocessor-controlled Lloyd (M 5K) materials testing instrument, loaded with a package of data analysis software (DAPMAT 3.0). Experiments were performed using a calibrated load cell of 1 kN at a crosshead speed of 10 mm min<sup>-1</sup> with an internal extensometer and automatic break detector having a constant gauge length of 25 mm throughout the tests. Samples were wrapped around the bollard before being clamped to the grip (TG12). The parameters such as the tensile strength, elongation, and work done at rupture before and after irradiation were measured. The values were calculated as an average of 10 measurements, and the results are presented with standard deviation for each type of sample.

**Chemical Resistance.** For this study, a small quantity of samples were irradiated up to a maximum dose of ~98 kGy at a dose rate of 1.0 kGy/h. The samples were dried, and their weight was recorded. The chemical solutions were prepared with two different concentrations of NaOH (5 and 1.25 mol L<sup>-1</sup>) and KMnO<sub>4</sub> (0.2 mol L<sup>-1</sup>) in deionized water. A sample of known weight (2 g) was treated with this solution

\* Corresponding e-mail: s.r.ahmad@cranfield.ac.uk.

<sup>†</sup> Current address: School of Chemistry, The University of Edinburgh, Kings Buildings, Edinburgh, EH9 3JJ, U.K.

for 1 h. The samples were rinsed in a 5% aqueous oxalic acid solution to remove any manganese dioxide and then washed in deionized water. Finally, the washed samples were dried in a vacuum at 40 °C, and their weight was recorded. The chemical resistance is measured by the weight difference of the same sample before and after chemical treatment according to the following equation:

$$\% \text{ weight loss} = \frac{W_{\text{un}} - W_{\text{chem}}}{W_{\text{un}}} \times 100 \quad (1)$$

where  $W_{\text{chem}}$  and  $W_{\text{un}}$  are the dry weight after and before chemical treatment.

**Fluorescence Spectroscopy.** A spectrofluorometer (FluoroMax SPEX Instruments) was used for fluorescence measurements. The fluorescence was detected at an angle of 90° signal collection geometry. The stray-light rejection factor of the detection monochromator is quoted to be  $\geq 10^3$  at  $\pm 5$  nm from the excitation line. Samples of 0.2 mg of size  $< 2$   $\mu\text{m}$  in length were compressed using a die pressed for 10 min at a pressure of 8 tons. The disk thus produced was inserted into a tightly fitting hole on a metal plate in the sample chamber of the spectrofluorometer. This arrangement ensured a fairly uniform irradiation over the surface of the sample, which is accurately reproducible. The spectra were recorded over the wavelength range 365–600 nm with a resolution of  $\pm 1$  nm at an excitation wavelength of 350 nm for three samples of each category, and an average was obtained.

**ATR-IR Spectroscopy.** The infrared spectra were recorded at room temperature using an ATR spectrometer (Graseby Specac, P/N 11209) having a resolution of  $\pm 3$  nm. Samples weighing 2 mg and  $< 2$   $\mu\text{m}$  in length were dispersed with 200 mg of dehydrated KBr and compressed into transparent tablets. The background spectral signal emanating from reflection, scattering, and fluorescence from the sample holder were recorded and subtracted from the spectral signal from the samples in holders. The intensities of bands were calculated as an average of three measurements for each type of sample with the same thickness, and the results are presented with standard deviations.

**Thermal Analysis.** For this, a TA 2010 differential scanning calorimeter (DSC) was used at a heating rate of 10 °C  $\text{min}^{-1}$  under nitrogen flow (50 mL  $\text{min}^{-1}$ ). The DSC instrument was calibrated for temperature and energy with indium and tin reference samples. DSC thermograms were recorded with about 5 mg of sample. Thermogravimetric (TGA) analysis was conducted using a Mettler TG 50 instrument. The measurements were taken over the temperature range 20–500 °C at 10 °C  $\text{min}^{-1}$ . TGA measurements were taken in nitrogen environment. The weight losses at each decomposition step, the decomposition temperatures, and the residue at each step were evaluated.

**X-ray Diffraction.** Powder wide-angle X-ray spectra were recorded from  $2\theta = 2^\circ$  to  $2\theta = 50^\circ$  with a Philips PW 1710 equipped with a graphite monochromator in a diffracted beam and using Nickel-filtered Cu K $\alpha$  radiation at  $\lambda = 0.1542$  nm (40 kV, 40 mA). The MDI Data Scan 3.2 software (Materials Data, Inc.) was used for data collection. The fibers of about 0.2 g and size  $< 2$   $\mu\text{m}$  in length were compressed using a die pressed for 5 min at a pressure of 10 tons using a Carver laboratory press. The disk thus produced was inserted into a tightly fitting hole on a sample holder of the diffractometer. The results were analyzed using MDI Jade 5 to determine the crystallinity ( $X_c$ ), calculated

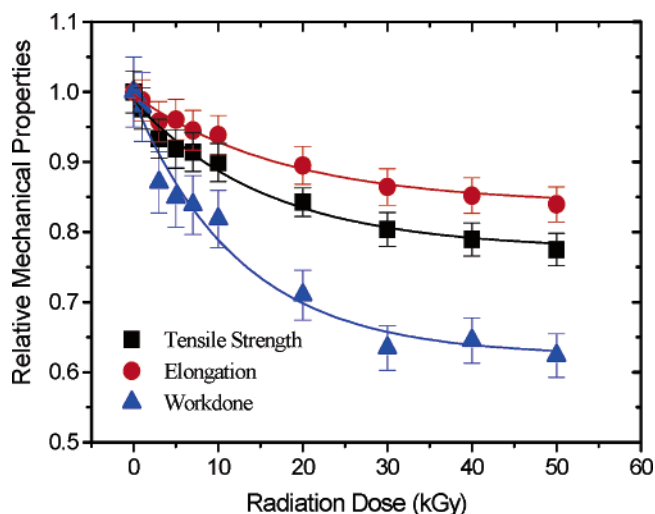


**Figure 1.** The mechanical properties plotted as a function of radiation dose. Samples were irradiated in the presence of air at a dose rate of 1.0 kGy/h.

as the ratio of the intensity under the crystalline peaks above the background to the total intensity.

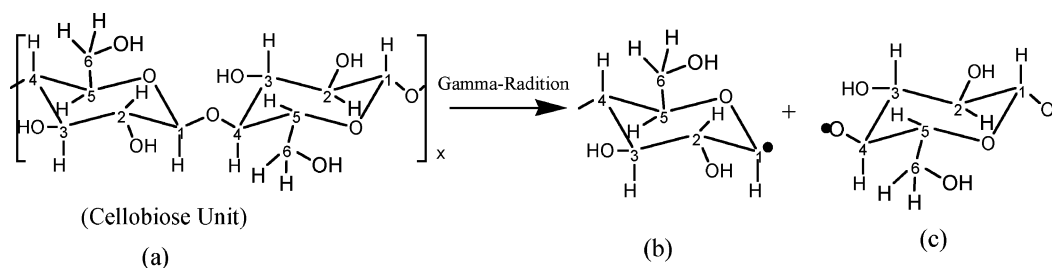
## Results and Discussion

**Mechanical Properties.** The mechanical properties are ascribed through the following parameters: tensile strength (TS), elongation at break (EB), and the corresponding work done (WD). These were plotted against the values of the corresponding radiation doses to which the sample was subjected in Figure 1. The TS, EB, and WD parameters were found to decrease by 22%, 16%, and 38%, respectively, with the increase of radiation dose for values up to 50 kGy. Since the effect, from a phenomenological consideration, is considered to correspond to first-order kinetics, all the curves were fitted to a modified Arrhenius equation of the following form:

$$Y_{\text{TS,EL,W}} = A + B \exp(-\lambda x) \quad (2)$$

where  $Y_{\text{TS,EL,W}}$  represents the tensile strength, elongation, and work done at rupture. The parameter  $x$  represents the radiation dose. The constant values obtained for tensile strength data are  $A = 0.77$ ,  $B = 0.22$ , and  $\lambda = 0.06$ ; for elongation at break,  $A = 0.81$ ,  $B = 0.18$ , and  $\lambda = 0.04$ ; and for work at rupture,  $A = 0.62$ ,  $B = 0.37$ , and  $\lambda = 0.08$ . The deterioration of mechanical properties of jute fiber characterized by the above parameters is attributed to a primarily radiation-induced chain scission reaction and, to a lesser extent, to some changes in the fibers' entanglement. The good fit of the data points to the above equation is an indication that the gross degradation of the above parameters, characterizing the mechanical properties of the cellulose, is caused by a first-order reaction process. This means

### Scheme 1. Chain Scission Reaction of Cellobiose Unit.



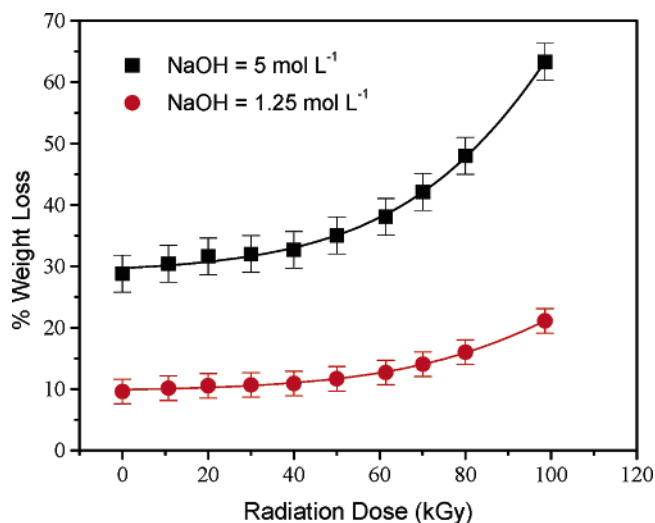


**Figure 2.** The effect of radiation dose on the chemical stability of jute fiber. Samples were irradiated in the presence of air at a dose rate of 1.0 kGy/h.

that the absorbed energy induces random chain scission in the cellulose chains which is proportional to the radiation dose. The present results on jute are found to be similar to those in other cellulose fibers, which had been attributed to a chain scission reaction<sup>5,18</sup> as described diagrammatically below. The radio-chemical reactions can occur at any carbon atom (i.e., C<sub>1</sub>–C<sub>6</sub>) by hydrogen and hydroxyl abstraction or C–C and C–O bond cleavage in the cellulose molecules (Scheme 1). Such reactions may also affect the mechanical properties of jute. In the presence of oxygen diffusion, the  $\gamma$ -radiation induced radicals in the cellulose materials also produce cellulose diperoxides (Cell–OO–Cell) and hydroperoxides (Cell–OOH) by a radical reaction process discussed elsewhere.<sup>14</sup> These peroxide species may also contribute to the degradation process. The radiation-induced chain scission reaction is represented in Scheme 1.

**Chemical Stability.** The chemical resistance of the irradiated samples was investigated according to the method described in

the Experimental Section. The soluble degradation products for different radiation doses were measured in terms of weight loss with 5 and 1.25 mol L<sup>−1</sup> of NaOH concentration and plotted in Figure 2. A weight loss of 10% was observed with 1.25 mol/L concentration of NaOH treatment for the nonirradiated sample. As the concentration of NaOH increased to 5 mol/L, the loss in weight was 29%. This is attributed to the slow dissolution of the low-molecular-weight lignocellulose chains. In both concentrations, the weight loss increases with radiation dose, and it is significantly higher above 50 kGy of radiation dose. This suggests that the radiation affected all anhydroglucose, hemicellulose, and lignin units, resulting in the fragmentation of molecules. More fragmentation of molecules is produced due to bond ruptures with the increase of radiation doses, which are more easily solubilized than the long-chain molecules. Thus, the chemical degradation increases with radiation doses.

High degradation of lignocellulose by a relatively small irradiation dose of  $\gamma$ -rays is attributed to the weakness of the chemical links between lignin, hemicellulose, and cellulose units. In lignocellulose material, the lignin is a structurally intricate aromatic polymer with oxygenated phenyl propane units, which is situated as filler between the highly ordered cellulose microfibrils. Upon exposure to  $\gamma$ -rays, the phenoxy radicals are most likely to produce and cause degradation on lignocellulose molecules.<sup>1</sup> When cellulose molecules are exposed to  $\gamma$ -rays, the radicals are produced in the cellulose chains as discussed before. Subsequently, these radicals are trapped in the crystalline and semicrystalline region of the cellulose structure. However, these radicals can decay through recombination reactions which lead to cross-linking. If the chain scission is predominant over cross-linking, the degradation on the properties is expected to be enhanced.<sup>5,6,8</sup>

**Fluorescence Property.** Fluorescence spectra of “as received” and irradiated samples (0–50 kGy at 1.0 kGy/h) are presented in Figure 3. The “as received” samples exhibit a broad-band emission spectrum with maximum at 455 nm. This broad emission band is attributed to the aromatic compounds or triene sequences in lignocellulose. On exposure to radiation,

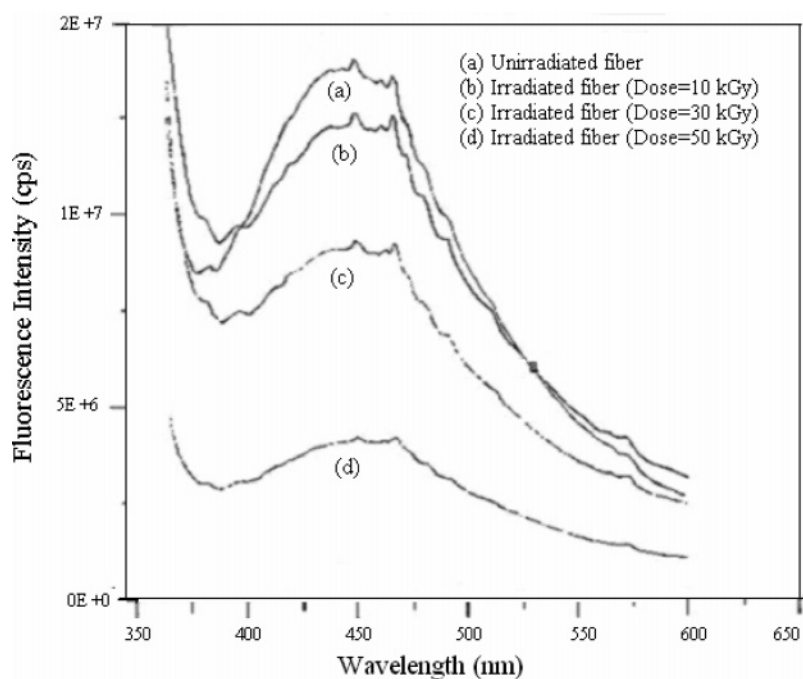


**Figure 3.** The fluorescence emission spectra of jute fiber “as received” and irradiated samples. Samples were irradiated in the presence of air at a dose rate of 1.0 kGy/h.



**Table 1.** Dependence of Fluorescence Parameters with  $\gamma$ -Radiation Dose at a Constant Intensity ( $1.0 \text{ kGy h}^{-1}$ )

radiation dose (kGy)	emission wavelength (nm)	relative integrated peak area	emission bandwidth (nm)	relative peak height
0	388–580	1.0	83.72	1.00
10	388–580	0.70	74.20	0.78
30	388–580	0.51	74.00	0.56
50	388–580	0.44	73.40	0.53

the spectral signatures remain unchanged (Figure 3b–d); however, the relative magnitude of fluorescence was found to decrease with the increase of radiation dose as shown in Table 1. For a total dose of 10 kGy, the peak intensity and the integrated area under the fluorescence band decreased by about 22% and 30%, respectively, and FWHM (full width at half-maximum) decreased by 11% while the peak wavelength positions remained unchanged. For higher radiation dose, e.g., 50 kGy, the reduction of the fluorescence integrated area is as much as 56% with a diminution of the peak intensity by about 47%; however, the bandwidth remains unchanged for doses above 10 kGy. The observed fluorescence properties of jute are found to be similar to those of cotton cellulose fibers.<sup>19–21</sup> Tylli et al.<sup>21</sup> observed a shaped peak with a maximum at 455 nm for pure cotton filter paper excited at 350 nm, which is in good agreement with our results. The assignments of fluorescence emission of other lignocellulose such as wood are well-documented,<sup>19–25</sup> although the source of the fluorescence emission has not been unequivocally identified. Oldstead and co-workers<sup>19,20</sup> have suggested that the observed fluorescence emission originates from the cellulose and the spectral characteristics are influenced by lignin acting as an inner filter. Several other published works<sup>22–24</sup> have interpreted that the fluorescence emission arises mainly from lignin chromophores in the lignocellulose fibers. The decrease in fluorescence with radiation dose indicates that the carbonyl groups are most likely to be produced in jute due to radiation in air, since it is known<sup>15–17</sup> that the irradiation of cellulose produces carbonyl and carboxyl groups and such groups tend to quench fluorescence emission.<sup>19–21</sup>

**ATR Infrared Analysis.** The IR spectral signature of the samples “as received” and irradiated are shown in Figure 4a. The spectrum of “as received” sample shows a strong absorption peak at  $714 \text{ cm}^{-1}$ , which is attributed to the out-of-plane C–H deformation vibrations of the hydrogen atoms remaining on the ring of aromatic component present in lignin. For irradiated samples, the peak at  $714 \text{ cm}^{-1}$  becomes weaker than the corresponding line for the “as received” sample. Characteristic broad absorption bands appeared in all samples having peaks at  $1100 \text{ cm}^{-1}$  with a shoulder at  $1032 \text{ cm}^{-1}$ , which are attributed to O–H deformation and C–O stretching vibrational modes. The O–H deformation mode also occurs at  $1225$  and  $1350 \text{ cm}^{-1}$  due to the phenolic hydroxyl group, as both these bands are sensitive to changes in the hydrogen-bonding pattern. The peaks at  $1431$  and  $1596 \text{ cm}^{-1}$  are attributed to the C–H deformation vibration. The C=O stretching of ester ketonic groups of the lignin can also be observed at  $1751$  and  $1838 \text{ cm}^{-1}$ . A well-defined absorption peak appeared at  $1921 \text{ cm}^{-1}$ , and several other strong absorption peaks at  $2054$ ,  $2134$ ,  $2210$ , and  $2455 \text{ cm}^{-1}$  appeared for all samples due to the hydrogen-bonded O–H stretching vibrations of chelate compounds. It was noticed that such bands become weaker for irradiated samples. The bands at  $3044$  and  $2968 \text{ cm}^{-1}$  are attributed to the intramolecular bonds of O–H and C–H stretching vibrations of the chelate in the crystalline region. In this region, a significant difference in

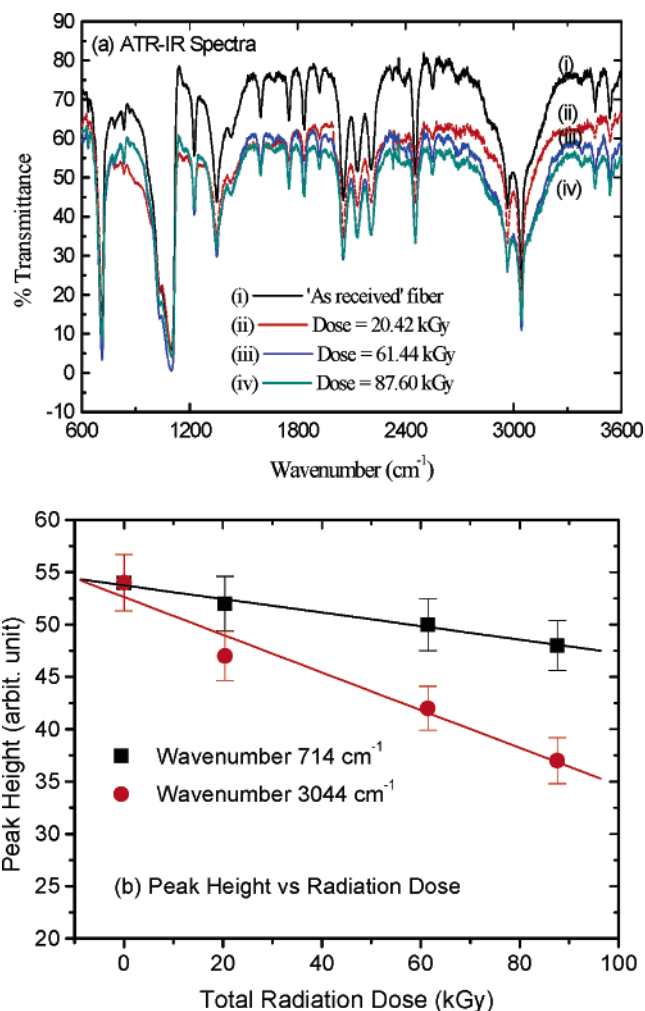


**Figure 4.** (a) Infrared spectra of “as received” jute fiber and irradiated samples. (b) Relative peak intensity versus radiation dose at  $714 \text{ cm}^{-1}$  and  $3044 \text{ cm}^{-1}$ . Samples were irradiated in the presence of air at a dose rate of  $1.0 \text{ kGy/h}$ .

intensity is seen (Figure 4a) with remaining the main peak position at  $3044 \text{ cm}^{-1}$ . The bands appeared between  $3400$  and  $3600 \text{ cm}^{-1}$  due to free OH groups at the C-2 and C-6 positions (Scheme 1) of cellulose molecules.<sup>20</sup>

Figure 4a shows that the radiation affected the intensity of all bands in the IR spectra. The intensities (i.e., peak height) for the bands at  $714$  and  $3044 \text{ cm}^{-1}$  as a function of radiation dose for the same thickness of the samples are plotted in Figure 4b. These bands follow first-order reaction kinetics so that the intensity ( $I$ ) is proportional to the population of the energy state in which the vibrating molecules exist. If these molecules exist in an energy level  $E_1$ , they can migrate to higher energy level  $E_2$  on excitation. The irradiation causes a decrease in the band's intensity (Figure 4b), which is attributed to the increasing energy barrier (e.g.,  $\Delta E = E_1 - E_2$ ) in the lignocellulose. It suggests that the vibrating groups that are responsible for the infrared bands undergo radiochemical changes by rupturing the chemical bonds and altering the molecular chain orientation, which are related to the energy barrier  $\Delta E$ .

**Thermal Analysis.** Figure 5 shows a comparison of DSC thermograms on “as received” and irradiated samples of jute fibers. The DSC thermogram of the “as received” jute fiber (Figure 5a, scan 1) shows an endotherm in the region between  $20$  and  $160 \text{ }^\circ\text{C}$ , with a minimum at  $90 \text{ }^\circ\text{C}$ . This is attributed to the characteristic water loss due to dehydration. In this region,

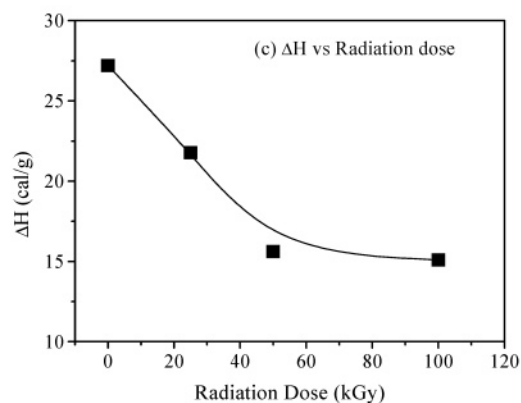
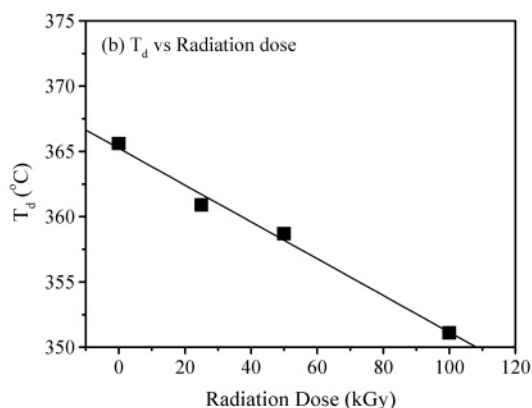
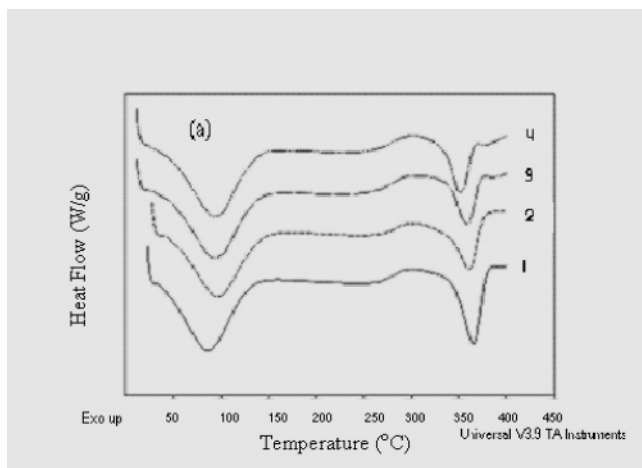


**Figure 5.** (a) DSC thermograms of “as received” fiber (1), irradiated fiber = 25 kGy (2), irradiated fiber = 50 kGy (3), and irradiated fiber = 100 kGy (4). (b)  $T_d$  versus radiation dose. (c)  $\Delta H$  versus radiation dose.

similar characteristic water loss behavior was also observed in the case of irradiated samples, with a minimum value at 93 °C. A tendency of endothermic reaction from 160 to 260 °C is seen for all samples, which is attributed to partial dehydration of the —OH primary groups and decomposition of minor constituents in jute. On further rise of the temperature up to 300 °C, an exothermic reaction was observed which is attributed to the decomposition of hemicelluloses. For the nonirradiated fiber, an endotherm in the range between 300 and 386 °C, having a peak minimum at 366 °C, was observed which represented the complete loss of —OH groups of the monomer units of cellulose and depolymerization and volatilization of cellulose.<sup>25–27</sup> For the jute samples irradiated to a total dose of 25 kGy, an endothermic peak between 300 and 385 °C, with a peak

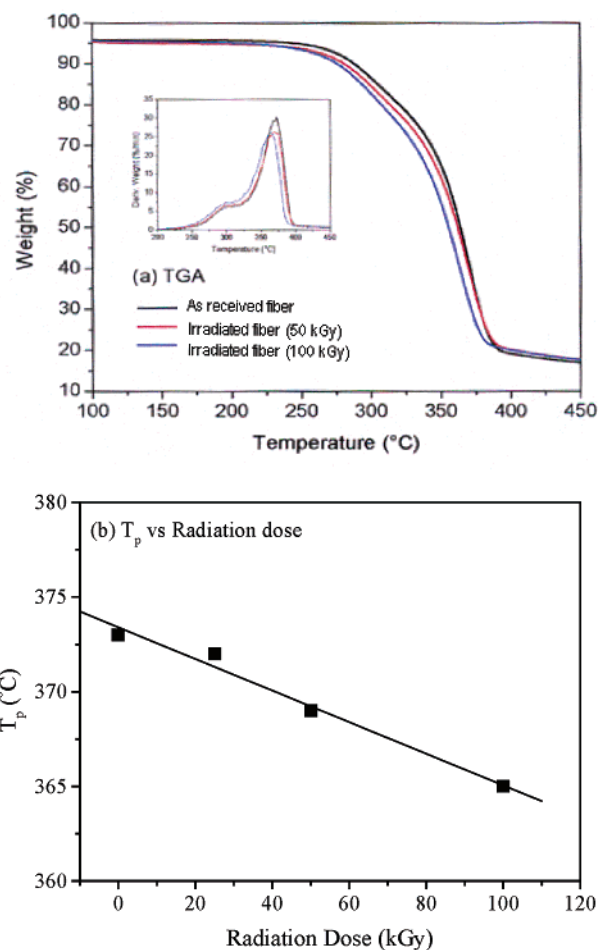


**Figure 6.** (a) TGA and DTG curves of samples “as received” and irradiated fiber. (b)  $T_p$  plotted as a function of irradiation dose of the jute fibers.

minimum at 361 °C (Figure 5a, scan 2), was observed. With increasing radiation dose, the endothermic peak became narrower, and the peak minimum (i.e., decomposition temperature,  $T_d$ ) reduced to 359 °C for 50 kGy and 351 °C for 100 kGy as plotted in Figure 5b. The calculated heat of fusion for the cellulose decomposition decreased linearly up to a radiation dose of 50 kGy, and for further increase of radiation dose, no significant change was observed (Figure 5c). The results show that the thermal stability of cellulose in jute decreases as the radiation dose increases.

The thermogravimetric (TG) and corresponding first derivative thermogravimetric (DTG) curves for the “as received” and irradiated jute fibers are shown in Figure 6a. The TGA graph of nonirradiated samples showed no weight loss in the range of temperature between 100 and 245 °C. The major weight loss occurred between 245 and 400 °C, which suggests the presence of a low molecular weight fragment, cleavage of glucosidal groups, and breakdown of anhydroglucose units in cellulose. In this case, there are two different regions of activities—the slow rate, between 245 and 315 °C, and the fast rate, between 315 and 400 °C (the latter marks active pyrolysis). The weight loss occurred in two steps corresponding to the peaks for “as received” and irradiated fiber. The first step represents the degradation of hemicelluloses, while the second step is due to the carbon residue and the degradation of cellulose. Concerning the main decomposition process, the temperatures  $T_i$  and  $T_f$  at which the decomposition begins and ends, respectively, and the decomposition temperature interval  $\Delta T = T_f - T_i$  have been

**Table 2.** Step Analysis Results of TGA of "as received" Sample and Irradiated Jute Fiber

radiation		TGA steps	$T_i$ (°C)	$T_f$ (°C)	$\Delta T = T_f - T_i$ (°C)	*WL (%)	residue (%)	$T_p$ (°C)
dose (kGy)								
0	I		245	315	70	13.2	81.8	373
	II		315	400	85	62.7	19.1	
25	I		245	315	70	13.4	82.0	372
	II		315	400	85	62.7	19.3	
50	I		220	310	90	13.6	81.4	369
	II		310	400	90	61.3	20.1	
100	I		205	305	100	14.0	81.0	365
	II		305	400	95	61.0	20.0	

evaluated. The decomposition weight loss has been calculated using the equation given below.

$$\% \text{ weight loss (WL)} = \frac{(m_i - m_r) \times 100}{m_i} \quad (3)$$

where  $m_i$  is the initial weight of the dry sample and  $m_r$  is the weight of the residue. The results are summarized in Table 2.

Results (Table 2) show that the decomposition temperature interval ( $\Delta T$ ) increases in the case of irradiated fiber. Although the weight loss and residue do not differ very much between nonirradiated and irradiated fibers, a noticeable difference is seen in the peak decomposition temperature. Figure 6b shows the peak temperature  $T_p$  at which the rate of degradation reaches the maximum value. In Figure 6b, it can be seen that the  $T_p$  (at  $10^\circ \text{C min}^{-1}$ ) decreases as the radiation dose of the sample increases. This suggests that the radiation, as expected, destroys the crystalline components of the samples, thereby making the samples more amenable to pyrolysis.

Pyrolytic degradation of the cellulose molecule may take place through cleavage of the glycosidic group or dehydration and breakdown of anhydroglucose units.<sup>26,27</sup> At lower temperatures, dehydration, elimination, and breakdown of sugar molecules take place, resulting in a gradual charring or depolymerization of the molecules. Reactions proceed slowly until around  $315^\circ \text{C}$ , when sufficient energy is available for a rapid cleavage of the glycosidic bond, the products evaporate, and levoglucosan and other tarry products are formed. Although the shapes of TGA curves of "as received" and irradiated samples do not differ very much from each other, a significant difference in  $T_p$  and  $\Delta T$  between "as received" and irradiated jute can be seen in DTG curves (Figure 6a).

**X-ray Diffraction.** Figure 7a summarizes the main structural changes observed in the wide-angle X-ray scattering (WAXS) spectra of the irradiated fibers. Only the spectral region where such changes appear ( $5^\circ < 2\theta < 30^\circ$ ) can be seen. Nonirradiated jute fibers display the typical X-ray pattern of cellulose I,<sup>28</sup> whereas the X-ray spectra of  $\gamma$ -irradiated samples gradually changed: the intensities of the crystalline peaks at  $2\theta = 10$ – $18^\circ$  and  $2\theta = 18$ – $30^\circ$  decreased. The overall crystallinity of irradiated fibers was estimated to have decreased from 42% to 31% for 100 kGy of irradiated dose, as shown in Figure 7b. This indicates that the high-energy radiation affected the cellulose structure significantly, resulting in changes of the other physical and chemical properties.

## Conclusions

From the analysis of the results, some specific conclusions are derived from the changes observed in the parameters

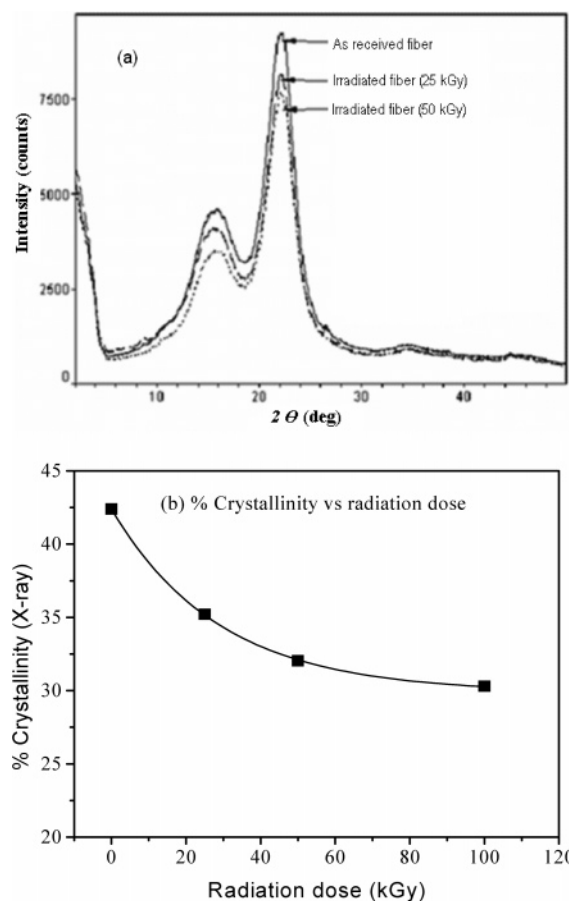


**Figure 7.** (a) WAXS spectra of "as received" and irradiated fiber (25 and 50 kGy). (b) The calculated crystallinity plotted as a function of radiation dose. Fibers were irradiated at room temperature at  $4.5 \text{ kGy h}^{-1}$ .

describing the mechanical characteristics of the lignocellulose fibers under investigation. The irradiation of jute by  $\gamma$ -radiation reduces the tensile strength, elongation, and work done at break. The changes in mechanical properties were significantly high up to 30 kGy of radiation dose. At this dose, the tensile strength was reduced by 20%, elongation by 14%, and work done at rupture by 37%. For further increase of radiation dose up to 50 kGy, the reduction in the above-mentioned mechanical parameters was not significant. This is attributed to the concurrent chain scission and cross-linking reactions taking place, especially at high radiation doses. The chemical stability decreases with radiation dose. The fluorescence properties of irradiated jute, both the peak and the integrated area under the peaks, were found to decrease with radiation dose. For 50 kGy of irradiated sample, the intensity of the band at 455 nm was reduced by 47% and the integral area by 56%. The decrease of fluorescence intensity with radiation dose suggests that radiochemical changes occurred in jute by  $\gamma$ -radiation, and the technique may be employed as a sensitive, nondestructive, and in situ method for characterization of lignocellulose polymer. Infrared spectral shape and signature showed significant changes caused by  $\gamma$ -radiation. The decrease in intensity with the increase of radiation dose could be attributed to the radiochemical changes in the lignocellulose molecules. Results of the thermal analysis (i.e., DSC and TGA) indicate that the thermal stability is lower in the case of irradiated samples than that without irradiated fiber. X-ray study showed a decrease in crystallinity upon exposure to  $\gamma$ -radiation indicating a structural change of lignocellulose caused by the radiation.

**Acknowledgment.** This research was partly funded by CEC under International Scientific and Technical Cooperation Scheme (INCO-DC).

## References and Notes

- (1) Khan, F. A. Radiation-Induced Graft Copolymerisation and Characterisation of Jute Fibre. Ph.D. Thesis, Cranfield University, U.K., 1999.
- (2) El-Nagar, A. M.; El-Hosamy, B. M.; Zahran, A. H.; Zohdy, M. H. *Am. Dyest. Rep.* **1992**, 81 (1), 40.
- (3) Williams, J. L.; Stannett, V.; Roldan, L. G.; Sello, S. B.; Stevens, C. V. *Int. J. Appl. Radiat. Isotopes* **1975**, 26, 169.
- (4) Charlesby, A. *Radiat. Phys. Chem.* **1981**, 18 (1–2), 59.
- (5) Campbell, F. J. *Radiat. Phys. Chem.* **1981**, 18 (1–2), 109.
- (6) Phillips, G. O.; Arthur, J. C., Jr. Photochemistry and Radiation Chemistry of Cellulose. In *Cellulose Chemistry and Its Applications*; Nevell, T. P., Zeronian, S. H., Eds.; Ellis Horwood Ltd. Publishers: Chichester, 1985; p 291.
- (7) Youssef, S. K.; Osiris, W. G.; Hashad, A. M. *Radiat. Phys. Chem.* **1996**, 47 (2), 321.
- (8) Wünderlich, K. *Radiat. Phys. Chem.* **1985**, 24 (5/6), 503.
- (9) Wilski, H. *Radiat. Phys. Chem.* **1987**, 29 (1), 1.
- (10) Leonhardt, J.; Arnold, G.; Baer, M.; Langguth, H.; Gey, M.; Huebert, S. *Radiat. Phys. Chem.* **1985**, 25 (4–6), 899.
- (11) Dziedziela, W. M.; Kotynska, D. J. *Radiat. Phys. Chem.* **1984**, 23 (6), 723.
- (12) Hill, D. J. T.; Hopewell, L. J. *Radiat. Phys. Chem.* **1996**, 48 (5), 533.
- (13) Sasuga, T.; Kawanishi, S.; Nishii, M.; Seguchi, T.; Kohno, I. *Radiat. Phys. Chem.* **1991**, 37 (1), 135.
- (14) Khan, F. *Macromol. Biosci.* **2005**, 5, 78–89.
- (15) Takács, E.; Wojnárovits, L.; Földvály, Cs.; Hargittai, P.; Borsa, J.; Sajó, I. *Radiat. Phys. Chem.* **2000**, 57, 399.
- (16) Takács, E.; Wojnárovits, L.; Borsa, J.; Földvály, Cs.; Hargittai, P.; Zöld, O. *Radiat. Phys. Chem.* **1999**, 55, 663.
- (17) Földvály, Cs. M.; Takács, E.; Wojnárovits, L. *Radiat. Phys. Chem.* **2003**, 67, 505.
- (18) Fischer, K.; Goldberg, W. *Macromol. Chem., Macromol. Symp.* **1987**, 12, 303.
- (19) Olmstead, J. A.; Gray, D. G. *J. Pulp Pap. Sci.* **1997**, 23, J571.
- (20) Olmstead, J. A.; Zhu, J. H.; Gray, D. G. *Can. J. Chem.* **1995**, 73, 1955.
- (21) Tylli, H.; Forsskahl, I.; Olkkonen, C. *Cellulose* **1996**, 3, 203.
- (22) Castellan, A.; Choudhury, H.; Davidson, R. S.; Grelier, S. *J. Photochem. Photobiol., A* **1994**, 81, 117.
- (23) Castellan, A.; Davidson, R. S. *J. Photochem. Photobiol., A* **1994**, 78, 275.
- (24) Machado, A. E. H.; Nicodem, D. E.; Ruggiero, R.; Perez, D. da S.; Castellan, A. *J. Photochem. Photobiol., A* **2001**, 138, 253.
- (25) Kondo, T. *Cellulose* **1997**, 4, 281.
- (26) Pandey, S. N.; Day, A.; Mathew, M. D. *Text. Res. J.* **1993**, 63 (3), 143.
- (27) Basak, R. K.; Saha, S. G.; Sarkar, A. K.; Saha, M.; Das, N. N.; Mukherjee, A. K. *Text. Res. J.* **1993**, 63, 658.
- (28) Marchessault, R. H.; Sundararajan, P. R. Cellulose. In *The Polysaccharides*; Aspinall, G. O., Ed.; Academic Press: New York, 1982; Vol. II, Chapter 2, p 11.

BM060168Y